INTERNATIONAL JOURNAL FOR NUMERICAL METHODS IN FLUIDS
Int. J. Numer. Meth. Fluids 2001; **37**: 107–123 (DOI: 10.1002/fld.170)

A multigrid approach for steady state laminar viscous flows

Shi-Jun Liao[a,*,1] and F. Mashayek[b]

[a] *School of Naval Architecture & Ocean Engineering, Shanghai Jiao Tong University, People's Republic of China*
[b] *Department of Mechanical Engineering, University of Illinois at Chicago, Chicago, USA*

SUMMARY

In this paper, we use the laminar viscous flow in a lid-driven cavity as an example to describe and verify a numerical scheme for non-linear partial differential equations. The proposed scheme combines a new analytical method for strongly non-linear problems, namely the homotopy analysis method, with the multigrid techniques. A family of formulas at different orders is given. At the lowest order, the current approach is the same as the traditional multigrid methods. However, our high-order scheme needs a fewer number of iterations and less CPU time than the classical ones. Copyright © 2001 John Wiley & Sons, Ltd.

KEY WORDS: multigrid technique; Navier–Stokes equations; viscous flow in a lid-driven cavity

1. INTRODUCTION

The multigrid method [1–3,20] is one of the most efficient numerical techniques for solving partial differential equations (PDE) and is widely applied in computational fluid dynamics (CFD) [4–10]. Multigrid techniques were first developed to solve linear PDEs. For linear PDEs, multigrid techniques are very efficient and can save a large amount of CPU time [1–3]. However, for non-linear PDEs such as Navier–Stokes equations in CFD, there often exist two kinds of coupled iterations, namely the inner and outer iterations. Owing to the non-linearity of viscous flow problems, the interaction between the inner and outer iterations is strong in general and therefore weakens the numerical efficiency of multigrid method.

In this paper, we propose a kind of non-linear multigrid technique by means of applying a new analytic technique for strongly non-linear problems, namely the homotopy analysis

* Correspondence to: School of Naval Architecture and Ocean Engineering, Shanghai Jiao Tong University, Shanghai 200030, People's Republic of China.
[1] E-mail: sjliao@mail.sjtu.edu.cn

Received January 2000
Revised April 2000

method (HAM) [11,12]. The HAM is proposed by one of the authors to overcome the restrictions and limitations of widely applied perturbation techniques. This method does not depend upon small parameters and provides us with great freedom to select proper base functions to approximate solutions of a non-linear problem. Liao [13] successfully applied the HAM to give, for the first time (to our knowledge), uniformly valid analytic solutions of some non-linear problems in fluid mechanics. Besides, the HAM has been successfully applied to develop some new numerical techniques, such as the general boundary element method [14–16] and so on [17]. Liao [17] verified that accurate enough numerical results of non-linear PDEs can be obtained even by means of no iterations. All of these verify the validity of the HAM in solving non-linear PDEs, and thus encourage us to further apply it to other non-linear problems in CFD.

As mentioned by Liao [12,13], the essence of the HAM is to transfer a non-linear problem into an infinite number of linear sub-problems and then to approximate the original non-linear problem by the solutions of the first several linear sub-problems. All of these linear sub-problems are governed by the same linear operator and therefore can be easily solved by numerical techniques, as mentioned by Liao [14–17]. Obviously, one can use multigrid techniques to solve these linear sub-problems so as to increase the numerical efficiency. In this paper, we combine the HAM with multigrid techniques to develop a new multigrid scheme for non-linear problems. We consider here the steady state laminar viscous flow in a driven cavity, governed by the dimensionless Navier–Stokes equations written in the vorticity ω and streamfunction ψ as follows:

$$\nabla^2\omega = Re\left(\frac{\partial\psi}{\partial y}\frac{\partial\omega}{\partial x} - \frac{\partial\psi}{\partial x}\frac{\partial\omega}{\partial y}\right) \tag{1.1}$$

$$\nabla^2\psi + \omega = 0 \tag{1.2}$$

and the boundary conditions

$$\psi = 0, \qquad \frac{\partial\psi}{\partial y} = 1, \qquad y = 1 \tag{1.3}$$

$$\psi = 0, \qquad \frac{\partial\psi}{\partial y} = 0, \qquad y = 0 \tag{1.4}$$

$$\psi = 0, \qquad \frac{\partial\psi}{\partial x} = 0, \qquad x = 0, \quad x = 1 \tag{1.5}$$

where Re is the Reynolds number. The spatial domain geometry and boundary conditions are as shown in Figure 1. This is a classical problem in CFD for testing new numerical techniques and therefore is a good starting point for us to develop and verify our multigrid scheme for non-linear PDEs.

2. THE BASIC IDEAS

Let $L(\omega, \psi)$ denote a two-dimensional linear partial differential operator, $\omega_0(x, y)$ and $\psi_0(x, y)$ the given (selected) initial guess solutions of the vorticity and streamfunction, respectively. Let $\eta_\omega,\ \eta_\psi,\ \eta_b$ be non-zero parameters and $p \in [0, 1]$ be a real number. We construct a set of PDEs

$$(1-p)\{L[W(x,y,p),\ \Psi(x,y,p)] - L[\omega_0(x,y),\ \psi_0(x,y)]\}$$
$$= p\eta_\omega \left\{ \nabla^2 W(x,y,p) - Re\left[\frac{\partial \Psi(x,y,p)}{\partial y} \frac{\partial W(x,y,p)}{\partial x} - \frac{\partial \Psi(x,y,p)}{\partial x} \frac{\partial W(x,y,p)}{\partial y} \right] \right\} \tag{2.1}$$

$$(1-p)[\nabla^2 \Psi(x,y,p) + W(x,y,p) - (\nabla^2 \psi_0 + \omega_0)] = p\eta_\psi [\nabla^2 \Psi(x,y,p) + W(x,y,p)] \tag{2.2}$$

and the boundary conditions

$$(1-p)[\Psi(x,y,p) - \psi_0(x,y)] = \eta_b p \Psi(x,y,p), \quad \text{when } x = 0 \text{ or } x = 1 \text{ or } y = 0 \text{ or } y = 1 \tag{2.3}$$

$$(1-p)\left[\frac{\partial \Psi(x,y,p)}{\partial y} - \frac{\partial \psi_0(x,y)}{\partial y} \right] = \eta_b p \left[\frac{\partial \Psi(x,y,p)}{\partial y} - 1 \right], \quad \text{when } y = 1 \tag{2.4}$$

$$(1-p)\left[\frac{\partial \Psi(x,y,p)}{\partial y} - \frac{\partial \psi_0(x,y)}{\partial y} \right] = \eta_b p \frac{\partial \Psi(x,y,p)}{\partial y}, \quad \text{when } y = 0 \tag{2.5}$$

$$(1-p)\left[\frac{\partial \Psi(x,y,p)}{\partial x} - \frac{\partial \psi_0(x,y)}{\partial x} \right] = \eta_b p \frac{\partial \Psi(x,y,p)}{\partial x}, \quad \text{when } x = 0 \text{ or } x = 1 \tag{2.6}$$

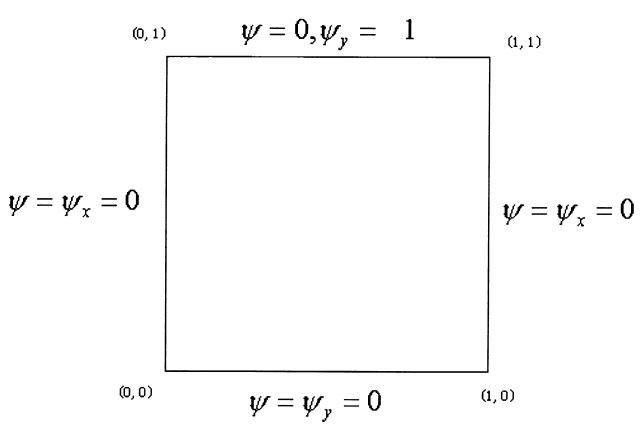

Figure 1. Spatial domain geometry and boundary conditions.

Assume that the auxiliary linear operator L, the auxiliary non-zero parameters $\eta_\omega,\ \eta_\psi,\ \eta_b$ and the initial guess solutions $\omega_0(x, y),\ \psi_0(x, y)$ are properly selected so that Equations (2.1)–(2.6) have solutions $W(x, y, p),\ \Psi(x, y, p)$ for $p \in [0, 1]$. Then, when $p = 0$, we have from Equations (2.1)–(2.6) that

$$W(x, y, 0) = \omega_0(x, y), \qquad \Psi(x, y, 0) = \psi_0(x, y) \tag{2.7}$$

When $p = 1$, Equations (2.1)–(2.6) are exactly the same as Equations (1.1)–(1.5). Thus, it holds

$$W(x, y, 1) = \omega(x, y), \qquad \Psi(x, y, 1) = \psi(x, y) \tag{2.8}$$

Therefore, as p increases from zero to one, $W(x, y, p)$ varies from the initial guess solution $\omega_0(x, y)$ to the solution $\omega(x, y)$, so does $\Psi(x, y, p)$ from $\psi_0(x, y)$ to $\psi(x, y)$. This kind of variation is called deformation in topology, so Equations (2.1)–(2.6) are named zero-order deformation equations. If the deformations $W(x, y, p)$ and $\Psi(x, y, p)$ are smooth enough so that they have the following derivatives at any order:

$$\omega_0^{[k]}(x, y) = \left.\frac{\partial^k W(x, y, p)}{\partial p^k}\right|_{p=0}, \quad k = 1, 2, 3 \ldots \tag{2.9}$$

$$\psi_0^{[k]}(x, y) = \left.\frac{\partial^k \Psi(x, y, p)}{\partial p^k}\right|_{p=0}, \quad k = 1, 2, 3 \ldots \tag{2.10}$$

we have via Equation (2.7) the corresponding Maclaurin series

$$W(x, y, p) = \omega_0(x, y) + \sum_{k=1}^{+\infty} \omega_k(x, y) p^k \tag{2.11}$$

$$\Psi(x, y, p) = \psi_0(x, y) + \sum_{k=1}^{+\infty} \psi_k(x, y)\, p^k \tag{2.12}$$

where

$$\omega_k(x, y) = \left.\frac{1}{k!}\frac{\partial^k W(x, y, p)}{\partial p^k}\right|_{p=0} \tag{2.13}$$

$$\psi_k(x, y) = \left.\frac{1}{k!}\frac{\partial^k \Psi(x, y, p)}{\partial p^k}\right|_{p=0} \tag{2.14}$$

If Equations (2.11) and (2.12) are convergent, we obtain by Equation (2.8) that

$$\omega(x, y) = \omega_0(x, y) + \sum_{k=1}^{+\infty} \omega_k(x, y) \tag{2.15}$$

$$\psi(x, y) = \psi_0(x, y) + \sum_{k=1}^{+\infty} \psi_k(x, y) \tag{2.16}$$

To give the governing equations and boundary conditions of $\omega_k(x, y)$ and $\psi_k(x, y)$, we first of all differentiate each of the zero-order deformation equations (2.1)–(2.6) k times and then set $p = 0$ and finally divide each side of them by $k!$. In this way, we get the so-called kth-order deformation equations ($k = 1, 2, 3 \ldots$)

$$L[\delta_k^{\omega}(x, y), \delta_k^{\psi}(x, y)] = \eta_{\omega} R_{\omega,k}(x, y) \tag{2.17}$$

$$\nabla^2[\delta_k^{\psi}(x, y)] + \delta_k^{\omega}(x, y) = \eta_{\psi} R_{\psi,k}(x, y) \tag{2.18}$$

and related boundary conditions

$$\delta_k^{\psi}(x, y) = \eta_b \psi_{k-1}(x, y), \quad \text{when } x = 0 \text{ or } x = 1 \text{ or } y = 0 \text{ or } y = 1 \tag{2.19}$$

$$\frac{\partial}{\partial y}[\delta_k^{\psi}(x, y)] = \eta_b \left[\frac{\partial \psi_{k-1}(x, y)}{\partial y} - (1 - \lambda_k) \right], \quad \text{when } y = 1 \tag{2.20}$$

$$\frac{\partial}{\partial y}[\delta_k^{\psi}(x, y)] = \eta_b \frac{\partial \psi_{k-1}(x, y)}{\partial y}, \quad \text{when } y = 0 \tag{2.21}$$

$$\frac{\partial}{\partial x}[\delta_k^{\psi}(x, y)] = \eta_b \frac{\partial \psi_{k-1}(x, y)}{\partial x}, \quad \text{when } x = 0 \text{ or } x = 1 \tag{2.22}$$

where

$$R_{\omega,k}(x, y) = \nabla^2 \omega_{k-1}(x, y) - Re \sum_{j=0}^{k-1} \left[\frac{\partial \psi_j(x, y)}{\partial y} \frac{\partial \omega_{k-1-j}(x, y)}{\partial x} - \frac{\partial \psi_j(x, y)}{\partial x} \frac{\partial \omega_{k-1-j}(x, y)}{\partial y} \right] \tag{2.23}$$

$$R_{\psi,k}(x, y) = \nabla^2 \psi_{k-1} + \omega_{k-1} \tag{2.24}$$

with the following definitions:

$$\delta_k^{\omega}(x, y) = \omega_k(x, y) - \lambda_k \omega_{k-1}(x, y) \tag{2.25}$$

$$\delta_k^{\psi}(x, y) = \psi_k(x, y) - \lambda_k \psi_{k-1}(x, y) \tag{2.26}$$

$$\lambda_k = \begin{cases} 0, & \text{when } k = 1 \\ 1, & \text{when } k > 1 \end{cases} \tag{2.27}$$

As soon as $\delta_k^{\psi}(x, y)$, $\delta_k^{\omega}(x, y)$ are known, we have via Equations (2.25) and (2.26) that

$$\omega_k(x, y) = \delta_k^{\omega}(x, y) + \lambda_k \omega_{k-1}(x, y) \tag{2.28}$$

$$\psi_k(x, y) = \delta_k^{\psi}(x, y) + \lambda_k \psi_{k-1}(x, y) \tag{2.29}$$

Notice that the kth-order equations (2.17) and (2.18) and related boundary conditions (2.19)–(2.22) are linear if $\omega_i(x, y)$ and $\psi_i(x, y)$, $i = 0, 1, 2, 3 \ldots k-1$, are known. Using the given initial approximations $\omega_0(x, y)$ and $\psi_0(x, y)$, Equations (2.17) and (2.18) are solved for $\delta_1^{\omega}(x, y)$ and $\delta_1^{\psi}(x, y)$ first and then $\omega_1(x, y)$ and $\psi_1(x, y)$ are calculated from Equations (2.28) and (2.29). Then again using the known $\omega_1(x, y)$ and $\psi_1(x, y)$, Equations (2.17) and (2.18) are solved for $\delta_2^{\omega}(x, y)$ and $\delta_2^{\psi}(x, y)$, etc.

If we consider only the first m terms of Equations (2.15) and (2.16), we have the mth-order approximations

$$\omega(x, y) \approx \omega_0(x, y) + \sum_{k=1}^{m} \omega_k(x, y) \tag{2.30}$$

$$\psi(x, y) \approx \psi_0(x, y) + \sum_{k=1}^{m} \psi_k(x, y) \tag{2.31}$$

They provide us with the mth-order iterative formulae

$$\omega_0^{i+1}(x, y) \leftarrow \omega_0^i(x, y) + \sum_{k=1}^{m} \omega_k^i(x, y) \tag{2.32}$$

$$\psi_0^{i+1}(x, y) \leftarrow \psi_0^i(x, y) + \sum_{k=1}^{m} \psi_k^i(x, y) \tag{2.33}$$

where $i = 0, 1, 2, 3 \ldots$, denotes the iteration number.

Table I. Parameters used for the first-order scheme ($m = 1$)

Re	$\eta_\omega = \eta_\psi = \eta_b$	v_0	v_1
1000	−1	2	4
3200	−0.75	2	4
5000	−0.35	3	6
7500	−0.45	10	20

Table II. Parameters used for the second-order scheme ($m = 2$)

Re	$\eta_\omega = \eta_\psi = \eta_b$	v_0	v_1
1000	−1	2	4
3200	−1	2	4
5000	−0.50	3	6
7500	−0.25	5	10

Table III. Number of iterations for the first- and second-order scheme

Re	First-order scheme	Second-order scheme
1000	8	4
3200	30	11
5000	110	37
7500	117	80

Because the current approach is based on the HAM, it also provides us with great freedom to select the auxiliary linear operator L, the initial guess $\omega_0(x, y)$, $\psi_0(x, y)$ and the auxiliary parameters η_ω, η_ψ, η_b. As shown by Liao [11–14], this kind of freedom is the cornerstone of the validity of the HAM and related numerical methods. For example, by the HAM, one has freedom to select better auxiliary linear operators, initial guesses and auxiliary parameters to ensure the series (2.15) and (2.16) is convergent. If they are properly selected so that Equations (2.17)–(2.22) can be solved analytically, one can obtain analytic solutions (this is exactly the idea of the HAM). If they are properly selected so that Equations (2.17)–(2.22) can be solved by the traditional boundary element method, one is applying the so-called general boundary element method [14]. As mentioned by Liao [17], one can use other numerical techniques, such as the finite volume method (FVM), the finite difference method (FDM) and the finite element method (FEM) to solve these linear sub-problems. And obviously, one can employ some accelerating techniques to these linear sub-problems. The HAM transfers the original non-linear problem into a series of linear sub-problems. Obviously, it is much easier to solve linear PDEs than non-linear ones, and the multigrid method is rather efficient for solving linear PDEs. Thus, it is logical and natural to combine the HAM with the multigrid methods.

3. MULTIGRID APPROACH

If we use mth-order iterative formulae (2.32) and (2.33), we need to solve the first m linear PDEs (2.17)–(2.22) one after the other in order. Many numerical techniques can be applied. In this paper, the linear PDEs (2.17)–(2.22) are solved by the multigrid technique. Considering the simplicity in geometry of the driven-cavity flow, we use the FDM to solve Equations

Table IV. CPU time

Re	First-order scheme	Second-order scheme
1000	1 min 45 s	1 min 30 s
3200	5 min 7 s	3 min 27 s
5000	18 min 30 s	12 min 7 s
7500	35 min 32 s	26 min 3 s

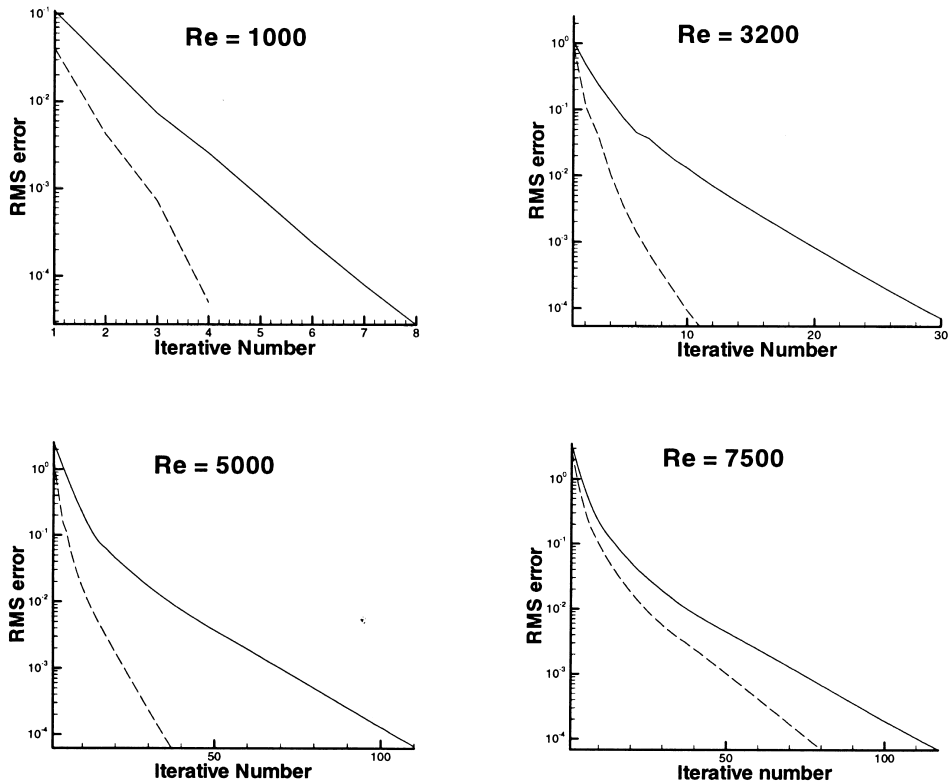

Figure 2. Root-mean-square errors via iteration number. Solid line: first-order scheme; dash line: second-order scheme.

(2.17)–(2.22) (one can also use the FVM, the FEM and so on in a similar way, if convenient). The related formulations are given as follows.

In this paper, we use

$$L(W, \Psi) = \nabla^2 W - Re\left(\frac{\partial \psi_0}{\partial y}\frac{\partial W}{\partial x} - \frac{\partial \omega_0}{\partial y}\frac{\partial \Psi}{\partial x}\right) \tag{3.1}$$

as our auxiliary linear operator, where $\omega_0(x, y)$, $\psi_0(x, y)$ are initial guess of streamfunction and vorticity. The high-order iterative formulae (2.28) and (2.29) are used. At each iteration, the calculated approximate results given by Equations (2.30) and (2.31) are used as new initial guess approximations to make the next iteration (outer iteration), as expressed by Equations (2.32) and (2.33). So, if the first-order ($m = 1$) iterative formulae (2.28) and (2.29) are applied and $\eta_\omega = \eta_\psi = \eta_b = -\rho$ is employed, where $\rho > 0$ is the relaxation parameter of the traditional successive overrelaxation (SOR) iterative method, the current approach is just the same as the

Table V. Comparisons of the results about primary vortex with those given by Ghia *et al.* [19]

Re	Current results				Results given by Ghia *et al.* [19]			
	$\psi_{\max}$	$\omega_{v,c}$	$x_{v,c}$	$y_{v,c}$	$\psi_{\max}$	$\omega_{v,c}$	$x_{v,c}$	$y_{v,c}$
1000	−0.1187	2.064	0.5313	0.5664	−0.1179	2.050	0.5313	0.5625
3200	−0.1209	1.945	0.5195	0.5393	−0.1204	1.989	0.5165	0.5469
5000	−0.1208	1.920	0.5156	0.5352	−0.1190	1.8602	0.5117	0.5352
7500	−0.1202	1.894	0.5117	0.5313	−0.1200	1.8799	0.5117	0.5322

traditional multigrid technique for laminar viscous flows. Thus, our approach logically contains some of the traditional iterative methods.

The essence of the multigrid method is to use a simple iterative technique as a smoother but not a solver to reduce the high-frequency components of errors on the current computational grid but to smooth out the low-frequency components of errors on coarser computational grids. For details, refer to [1–3,10]. Let G^k denote the series of computational grids, where $k = 0, 1, 2 \ldots M$. Here, G^0 denotes the coarsest grid, G^M the finest ones. For simplicity, uniform grid is used at each level of grid. Let h_k denote the step size on the grid G^k and $h_{k+1} = h_k/2$ hold. On the grid G^k, let $\omega^k_{i,j}$ and $\psi^k_{i,j}$ denote the vorticity and streamfunction at point (ih_k, jh_k). We use five-level grids, i.e. 257×257, 129×129, 65×65,33×33 and 17×17. The V-cycle multigrid scheme is applied. Following Wesseling [18], we use the nine-point restriction operator

$$
\begin{aligned}
&(R^{k-1}_k f^k)_{i+1,j+1} \\
&= \frac{1}{4} f^k_{2i+1,2j+1} + \frac{1}{8}\left(f^k_{2i+2,2j+1} + f^k_{2i+1,2j+2} + f^k_{2i,2j+1} + f^k_{2i+1,2j}\right) \\
&\quad + \frac{1}{16}\left(f^k_{2i+2,2j+2} + f^k_{2i,2j+2} + f^k_{2i+2,2j} + f^k_{2i,2j}\right)
\end{aligned} \tag{3.2}
$$

and the nine-point prolongation operator P^{k-1}_k defined by

$$(P^k_{k-1} f^{k-1})_{2i+1,2j+1} = f^{k-1}_{i+1,j+1} \tag{3.3}$$

$$(P^k_{k-1} f^{k-1})_{2i+2,2j+1} = \frac{1}{2}\left(f^{k-1}_{i+1,j+1} + f^{k-1}_{i+2,j+1}\right) \tag{3.4}$$

$$(P^k_{k-1} f^{k-1})_{2i+1,2j+2} = \frac{1}{2}\left(f^{k-1}_{i+1,j+1} + f^{k-1}_{i+1,j+2}\right) \tag{3.5}$$

$$(P^k_{k-1} f^{k-1})_{2i+2,2j+2} = \frac{1}{4}\left(f^{k-1}_{i+1,j+1} + f^{k-1}_{i+1,j+2} + f^{k-1}_{i+2,j+1} + f^{k-1}_{i+2,j+2}\right) \tag{3.6}$$

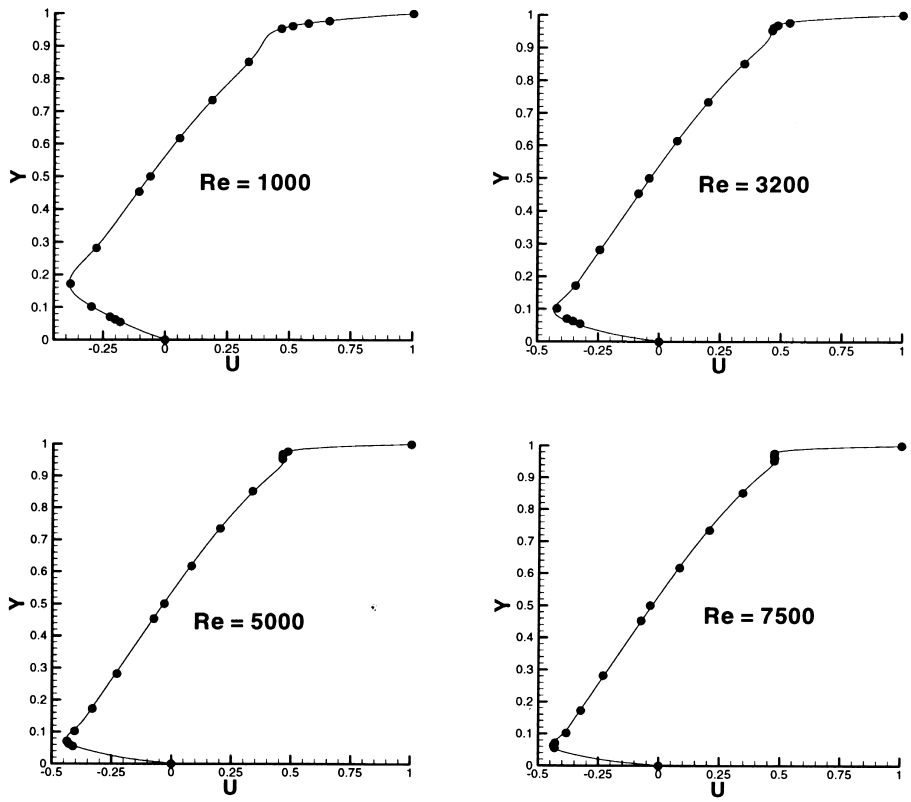

Figure 3. Profiles of velocity u at $x = 1/2$ for $Re = 1000$, 3200, 5000, 7500. Solid line: current result; solid circle: results given by Ghia *et al*. [19].

The SOR method is used as the smoothing operator S^v, where v denotes the number of the (inner) iterations. An ADI technique is employed. Second-order accurate central finite difference approximations are applied to all second-order derivatives in Equations (2.17) and (2.18). The convective terms are represented via a first-order accurate upwind difference scheme, but second-order accurate central-difference approximations are employed for all other first-order derivatives in Equations (2.17) and (2.18). Following Ghia [19], we use on the boundary ∂D the second-order accurate approximations

$$\nabla^2 f_J = \frac{1}{2h^2}\left[8f_{J-1} - f_{J-2} - 7f|_{\partial D} - 6h\left.\frac{\partial f}{\partial n}\right|_{\partial D}\right] \tag{3.7}$$

The corresponding boundary conditions (2.19)–(2.22) should be employed in the above expressions. The value of v for the operator S^v may be different at different grid G^k. On the

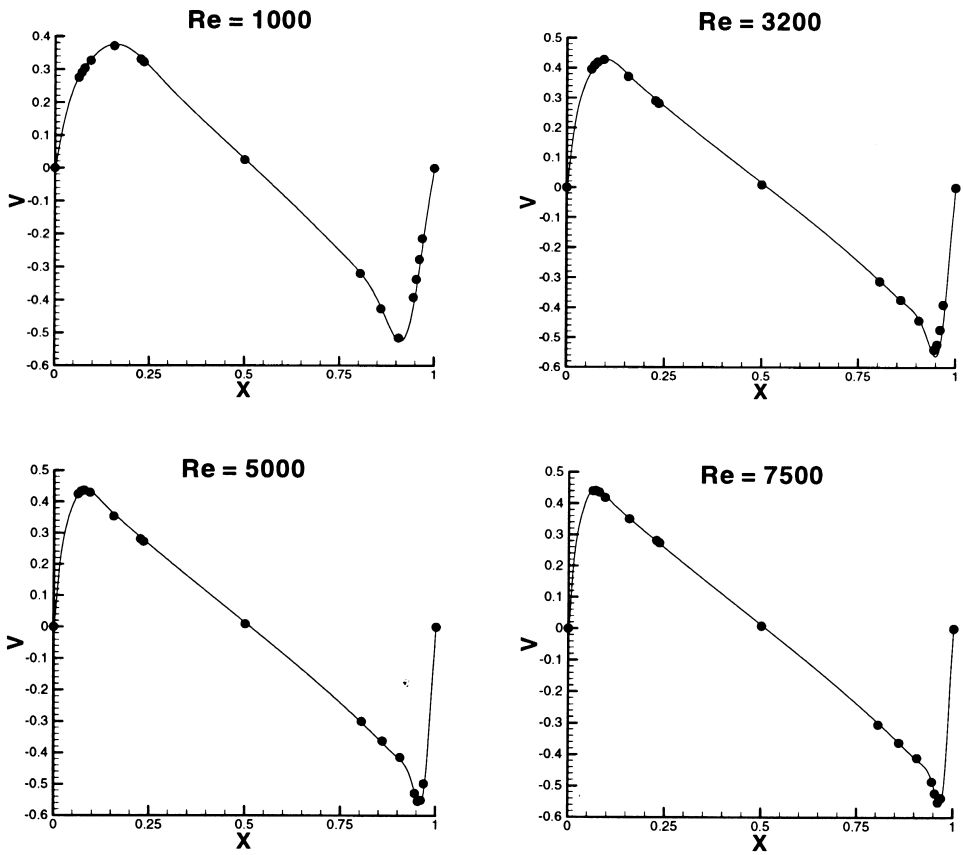

Figure 4. Profiles of velocity v at $y = 1/2$ for $Re = 1000$, 3200, 5000, 7500. Solid line: current result; solid circle: results given by Ghia *et al*. [19].

coarsest grid G^0, S^v is used as a solver so that v should be large enough to make the iteration convergent. On the other grids, S^v is employed as a smoother so that a few iterations are enough. In this paper, we set $v = v_0$ on the finest grid and $v = v_1$ on the other grids excluding the coarsest one.

Let $\mathbf{r}_0$, $\mathbf{r}_M$ denote the residuals of Equations (2.17) and (2.18) and related boundary conditions (2.19)–(2.22) on the coarsest grid G^0 and the finest grid G^M, respectively. Convergence is defined to occur when the Euclid norm of the residuals is below a specified tolerance. On the coarsest grid G^0, the convergence criterion is

$$\|\mathbf{r}_0\| < \frac{\|\mathbf{r}_M\|}{\alpha^M} \tag{3.8}$$

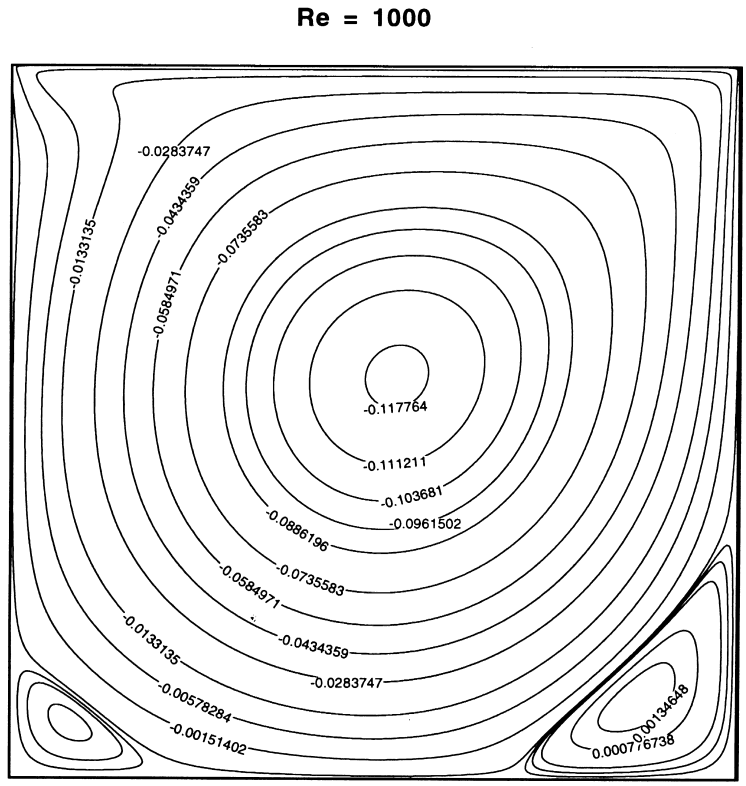

Figure 5. Contour of the streamfunction ψ when $Re = 1000$.

where $\alpha > 1$, and $\|\mathbf{r}_0\|$, $\|\mathbf{r}_M\|$ are the Euclid norms of the residuals $\mathbf{r}_0$ and $\mathbf{r}_M$, respectively. Let $\|\mathbf{r}_M^0\|$ denote the Euclid norm of the original equations for the initial guess approximations $\psi_0(x, y)$, $\omega_0(x, y)$ on the finest grid. The criterion for the finest grid is

$$\|\mathbf{r}_M\| < \frac{\|\mathbf{r}_M^0\|}{\beta} \tag{3.9}$$

where $\beta > 1$. The final result is obtained when the Euclid norm of the residual $\mathbf{r}_M$ is less than 10^{-4}. Notice that the iterative times on the coarsest grid G^0 are determined by the convergence criterion (3.8); however, the iterative times on the other grids are fixed, i.e. v_0 on the finest grid but v_1 on the other grids excluding the coarsest one.

We employ the traditional V-cycle multigrid technique to solve m linear sub-problems governed by Equations (2.17)–(2.22).

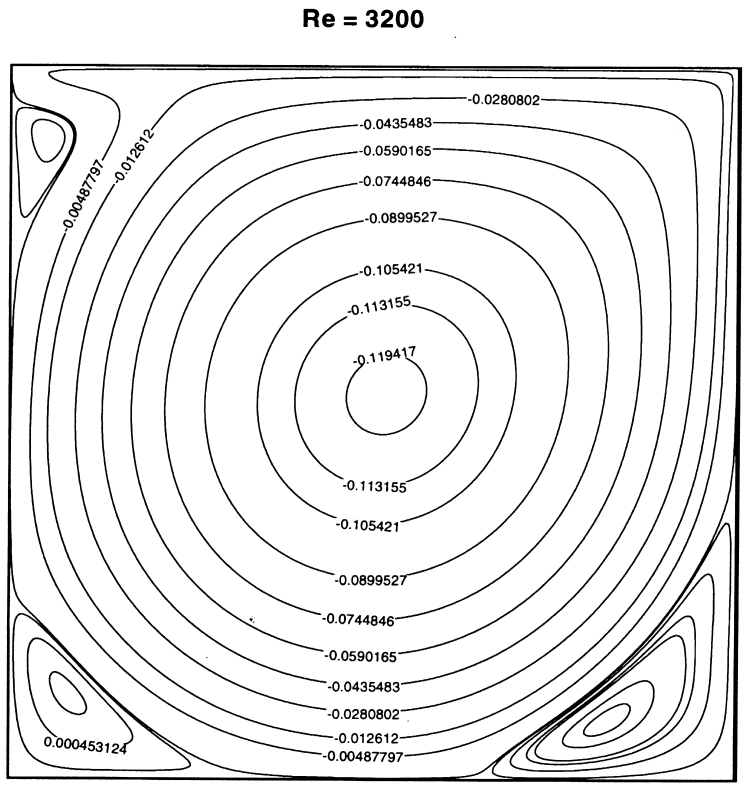

Figure 6. Contour of the streamfunction ψ when $Re = 3200$.

4. NUMERICAL RESULTS

Equations (2.32) and (2.33) provide us with a family of iteration formulae. However, as a starting point, in this paper we only consider two kinds, i.e. $m = 1$ and $m = 2$. The former corresponds to the traditional multigrid method if we regard $\eta_\omega = \eta_\psi = \eta_b = -\rho$, where ρ is the relaxation parameter of traditional SOR method (for outer iterations). The latter is the second-order scheme of our current approach. Thus, we can compare the current approach with traditional multigrid methods.

In this paper, four Reynolds numbers, $Re = 1000,\ 3200,\ 5000,\ 7500$, are considered. In all cases we use $\alpha = 2$, $\beta = 5$ and set all relaxation parameters of the smoother S^v (inner iterations) on all grids to be 0.25. The values of $\eta_\omega = \eta_\psi = \eta_b$ and v_0, v_1 for first- and second-order schemes are shown in Table I ($m = 1$) and Table II ($m = 2$), respectively. The corresponding iteration number and related CPU times are given in Tables III and IV, respectively. The curves of root-mean-square errors via the iteration number for the first- and second-order

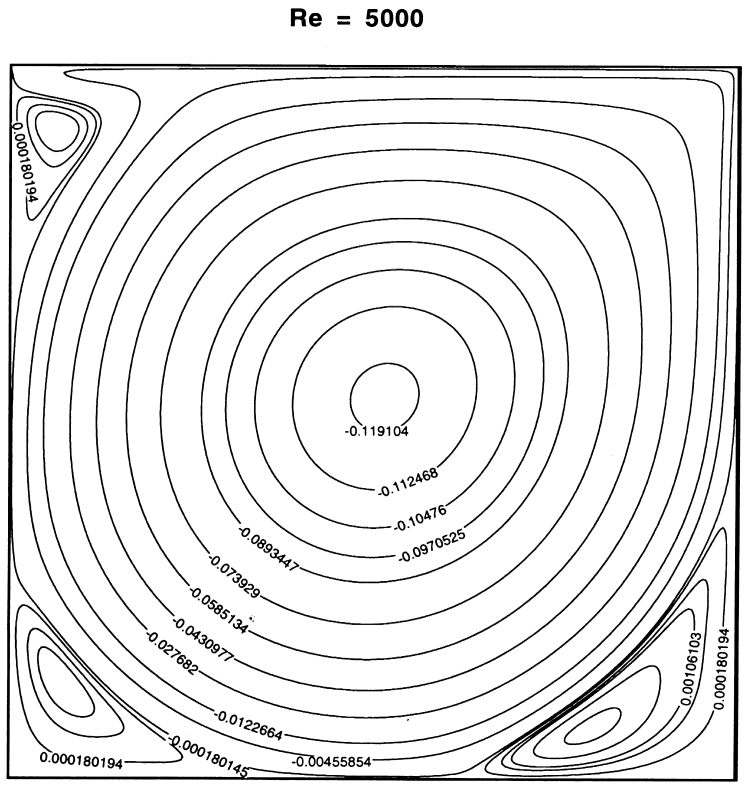

Figure 7. Contour of the streamfunction ψ when $Re = 5000$.

schemes are as shown in Figure 2. From Table III and Figure 2, the second-order formula needs less iteration in all cases. Liao [14–17] reported the same results in some other problems without using multigrid methods. Thus, this result has general meanings. From Table IV, the second-order scheme ($m = 2$) needs even less CPU time in all cases than the first-order scheme ($m = 1$) that corresponds to the traditional multigrid technique. This is because the second-order scheme gives more accurate results than the first-order one and therefore accelerates the iterations. Another reason might be that there exist strong, complicated, interactions between inner and outer iterations of the multigrid method. Note that in the case of $Re = 5000$, the first-order formula diverges when $\eta_\omega = \eta_\psi = \eta_b = -0.5$ and therefore we had to decrease the absolute value of $\eta_\omega = \eta_\psi = \eta_b$ to make the iteration convergent. Besides, in the case of $Re = 7500$ and $v_0 = 5$, $v_1 = 10$, the first-order formula diverges and we had to increase the iteration numbers at each grid level to make the iteration convergent. These verify that our second-order approach seems more stable and converges faster than the traditional multigrid method.

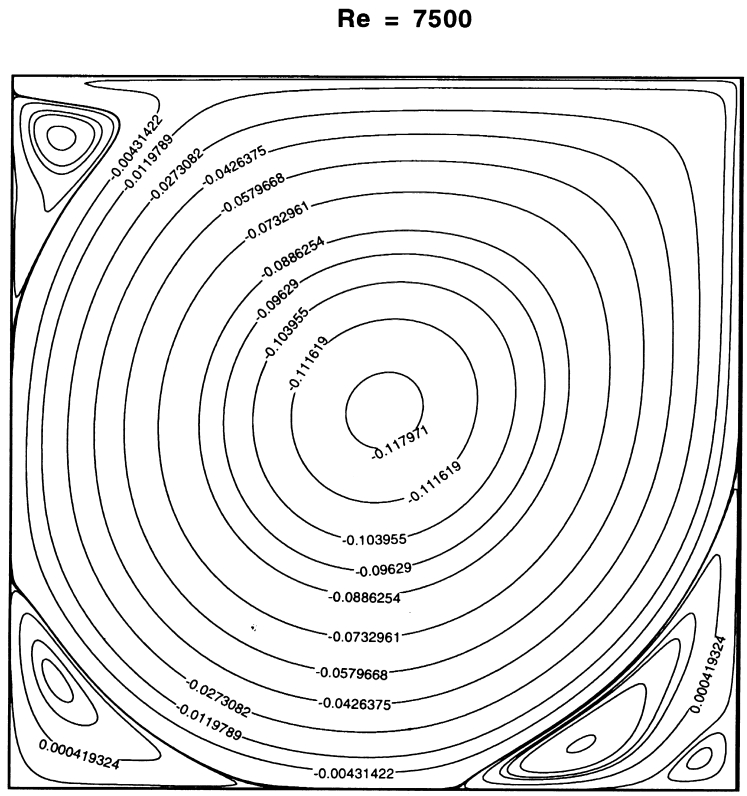

Figure 8. Contour of the streamfunction ψ when $Re = 7500$.

The comparions of the center of the primary vortex, the values of vorticity and streamfunction there, with those reported by Ghia *et al.* [19], are given in Table V. Besides, the velocity profiles of u at $x = 1/2$ and v at $y = 1/2$, compared with the results given by Ghia *et al.* [19] are shown in Figures 3 and 4, respectively. The contours of the streamfunction ψ are shown in Figures 5–8. All of these agree well with numerical results given by Ghia *et al.* [19]. Therefore, our numerical results are reasonable.

5. CONCLUSIONS

In this paper, encouraged by the successful applications of a new kind of analytic technique, namely the HAM, we further apply the basic ideas of this new analytic method to propose a new numerical scheme for non-linear PDEs. By combining the HAM with the multigrid techniques, we present a new multigrid scheme for laminar viscous flow problems governed by the Navier–Stokes equations in the form of streamfunction ψ and vorticity ω. At the lowest

order ($m = 1$), our approach is the same as the traditional multigrid method, so that it logically contains the traditional ones (this is similar to the fact that the so-called general boundary element method [14,15] contains the traditional boundary element method). Our calculations show that the high-order ($m = 2$) scheme seems more stable and converges faster than the traditional multigrid method. Therefore, the development of some more efficient and stable multigrid schemes for complicated viscous flow problems in CFD seems promising.

Notice that, with comparison to practical viscous flows, the driven-cavity viscous flow is very simple. Thus, the validity of the proposed approach should be further assessed by applying it to other more complicated three-dimensional viscous problems governed by the Navier–Stokes equations in primitive variables. Notice that there exist many auxiliary parameters in our approach, such as η_ω, η_ψ, η_b and so on, and it is interesting to investigate if they have optimal values and how to determine them if the answer is positive. Notice also that in this paper Equation (3.1) is employed as our auxiliary linear operator L. As pointed out by Liao [12,13], the current approach provides us with great freedom to select the auxiliary linear operator L and therefore many other linear operators might be possible. It would be interesting to research how to select an optimal one from all these possible linear operators. All of these problems are worth further investigations, as mentioned by Liao [12,13].

ACKNOWLEDGMENTS

The authors would like to thank the reviewers for their valuable comments and suggestions.

REFERENCES

1. Brandt A. Guide to multigrid development. In *Multigrid Methods: Lecture Notes in Mathematics*, vol. 960, Hackbusch W, Trottenberg U (eds). Springer-Verlag: Berlin, 1982; 220–312.
2. Brandt A. Multi-level adaptive solutions to boundary-value problems. *Mathematics and Computing* 1977; **31**: 333.
3. Brandt A, Yavneh I. Accelerating multigrid convergence and high-Reynolds recirculating flows. *SIAM Journal of Scientific Computing* 1993; **14**: 607.
4. Gjesdal T, Lossiue M E H. Comparison of pressure correction smoothers for multigrid solution of incompressible flow. *International Journal for Numerical Methods in Fluids* 1997; **25**: 393.
5. Lavery N, Taylor C. Iterative and multigrid methods in the finite element solution on incompressible and turbulent fluid flow. *International Journal for Numerical Methods in Fluids* 1999; **30**: 609.
6. Lien FS, Leschziner MA. Multigrid acceleration for turbulent flow with a non-orthogonal collocated scheme. *Computer Methods in Applied Mechanics and Engineering* 1994; **118**: 351.
7. Paisley MF. Multigrid computation of stratified flow over two-dimensional obstacles. *Journal of Computational Physics* 1997; **136**: 411.
8. Thompson MC, Ferziger JH. An adaptive multigrid technique for the impressible Navier–Stokes equations. *Journal of Computational Physics* 1989; **82**: 94.
9. Xia J, Taylor C. A multigrid solution based on the FEM for the Navier–Stokes equations. *Engineering and Computers* 1992; **9**: 469.
10. Zeng S, Wesseling P. Multigrid solution of the incompressible Navier–Stokes in generalized coordinates. *SIAM Journal of Numerical Analysis* 1994; **31**: 1764.
11. Liao SJ. A approximate solution technique which does not depend upon small parameters (Part 2): an application in fluid mechanics. *International Journal of Non-Linear Mechanics* 1997; **32**(5): 815–822.
12. Liao SJ. An explicit, totally analytic approximation of Blasius' viscous flow problems. *International Journal of Non-Linear Mechanics* 1999; **34**(4): 759–778.
13. Liao SJ. A uniformly valid analytic solution of 2D viscous flow past a semi-infinite flat plate. *Journal of Fluid Mechanics* 1999; **385**: 101–128.
14. Liao SJ. On the general boundary element method and its further generalizations. *International Journal of Numerical Methods for Fluids* 1999; **31**: 627–655.

15. Liao SJ, Chwang AT. General boundary element method for unsteady non-linear heat transfer problems. *International Journal of Numerical Heat Transfer B Fundamental* 1999; **35**(2): 225.
16. Liao SJ. On the general boundary element method. *Engineering Analysis with Boundary Elements* 1998; **21**(1): 39–51.
17. Liao SJ. Numerically solving non-linear problems by the homotopy analysis method. *Computational Mechanics* 1997; **20**(6): 530–540.
18. Wesseling P. Theoretical and practical aspects of a multigrid method. Report NA-37, Delft University of Technology, The Netherlands, 1980.
19. Ghia U, Ghia K N, Shin C T. High-Re solutions for incompressible Navier–Stokes equations and a multi-grid method. *Journal of Computational Physics* 1982; **48**: 387.
20. Wesseling P. *An Introduction to Multigrid Methods. Pure and Applied Mathematics*. Wiley: Chichester, 1992.

